LAWRENCE
LIVERMORE
NATIONAL
LABORATORY

UCRL-TR-227085

Simple Common Plane contact algorithm for explicit FE/FD methods

Oleg Vorobiev

January 5, 2007

This work was performed under the auspices of the U.S. Department of Energy by University of California, Lawrence Livermore National Laboratory under Contract W-7405-Eng-48.

Simple Common Plane contact algorithm for explicit FE/FD methods

Oleg Vorobiev

Lawrence Livermore National Laboratory
L-206, P.O. Box 808, Livermore, CA 94550, USA

Abstract

Common-plane (CP) algorithm is widely used in Discrete Element Method (DEM) to model contact forces between interacting particles or blocks. A new simple contact algorithm is proposed to model contacts in FE/FD methods which is similar to the CP algorithm. The CP is defined as a plane separating interacting faces of FE/FD mesh instead of blocks or particles used in the original CP method. The new method does not require iterations even for very stiff contacts. It is very robust and easy to implement both in 2D and 3D parallel codes.

Introduction

Many materials and structures are discontinuous by nature. For example, rock masses include multiple joints and faults, granular materials are composed of small particles, buildings are composed of bricks etc. There are two types of methods to describe discontinuous media: implicit and explicit.

In the implicit methods discontinuities are contained within the elements and are characterized by additional variables. The simplest example is the Volume-Of-Fluid (VOF) method used to describe material interfaces in Eulerian hydrocodes [1]. Joints and faults in rocks present another type of discontinuities. Mechanical properties of joints are different from those for the material and their thickness is very small compared to the wave length in the problem. Such discontinuity can be treated as thin structures imbedded into continuum. Due to the presence of joints the total response of an element is a combination of solid and joint responses. In this case the stress update for the element may require iterations between the solid and joint components and overall response is anisotropic. For heavily jointed rock media the implicit approach is often reduced to the equivalent continuum models [3,4,5]. Such approach is useful when the total number of joints is very big.

The implicit methods become complicated when there are several sets of joints in the system so that each element contains differently oriented joints. One of the advantages of the implicit joint treatment is that there are no additional efforts required to parallelize the code. Yet, it may not be robust if deformations are large since the anisotropy of the element response may cause elements to distort, for example, along the sliding direction. Besides, the implicit treatment of discontinuities is not appropriate for contact-impact

problems, for example, when the blocks separate from each other and impact other blocks.

In the explicit methods the joints are represented either by thin-layer elements [6, 7] or by the contact interactions between the mesh boundaries. In either case the discontinuities are aligned along the mesh boundaries. The method using contact interactions is considered in the present paper. The interactions are modeled by adding contact forces which prevent the mesh boundaries from interpenetration.

The most popular approach for contact calculations in the explicit finite element analysis is the master-slave slide-line algorithm with the penalty method [8, 9]. In this method one of the interacting surfaces (master) serves as a boundary constraining the motion of the nodes for the other surface (slave). To prevent the penetration of a slave node through the master surface a penalty force proportional to the projected over-penetration is applied both to the slave node and with the opposite sign to the nodes of the master face. The direction of this force is usually defined by the normal to the master surface, which is discontinuous due to discretization of the boundary. This discontinuity causes oscillations at the contacts. More sophisticated methods have been developed to overcome this problem [10,11].

When master-slave approach is used, the user is expected to designate master and slave surfaces in advance before the start of calculations [12]. For better symmetry master and slave surfaces can alter each cycle [9,13]. The penalty method only approximately satisfies the contact displacement constraints and is sensitive to the value of the penalty coefficient controlled by the user. Small values of this coefficient can cause over penetration as a consequence a softer than needed contact response. Big values of the penalty coefficient can cause instability at the contact.

In many practical problems such as for the motion of heavily jointed rock masses the number of discontinuities is big. The accuracy of the modeling for these discontinuities may have a significant effect on overall response of the system. To reproduce the response of a single joint observed in experiments constitutive equations used to model contacts should be able to describe more than just simple Coulomb-type frictional sliding. The normal stiffness can be very non-linear and the shear strength typically shows initial hardening followed by dilatancy and softening [17]. Therefore effective contact detection algorithms with realistic mechanical models implemented for distributed-memory parallel computers become very important. Systems with multiple discontinuities can be effectively modeled with DEM methods. The DEM has been applied to model underground structure response to strong ground motion [21], multi-fracturing of solids [22], granular flow etc. One of the popular contact detection techniques in DEM, is the Common-plane algorithm introduced by Cundall [14]. This algorithm reduces the expensive object-to-object contact detection problem to a less expensive plane-to-object contact problem. Interacting objects are polygons in 2D case and polyhedral in 3D case. The Common Plane (CP) is defined as a plane bisecting the space between the objects. After CP has been determined each object is tested separately for contacts with the common-plane. The algorithm [14] was improved in [15] by adding a fast method to identify the right candidates for the common plane. DEM by nature are not designed to model continuum and, for this purpose, are very often supplemented by coupled FE codes [21]. Also, when subject to very intense shock loadings DEM with stiff

contacts cannot run effectively due to severe restrictions on time step imposed by the stability condition.

The algorithm described in the present paper has been designed to model multiple contacts in FE rather than DEM codes. Because it handles a more simple case, the interaction of two faces rather than blocks, it was called the Simple Common Plane contact algorithm or SCP. This algorithm has been implemented in a parallel 2D and 3D Lagrange FE code (GEODYN-L) for shared memory machines using MPI.

In addition to the traditional explicit algorithm for the stress update at Common Plane similar to one used in [14] a more advanced quasi-implicit update has been implemented to avoid strict time step limitations for the problems with stiff contacts.

GEODYN-L Computational Algorithm

GEODYN-L is a parallel explicit Lagrangian solver for 2D and 3D unstructured meshes. It supports simple 2D and 3D elements (QUADS, TETS, HEX) and multiple materials within the elements. Parallel implementation of GEODYN-L can be summarized as follows:

- The code does not use globally defined connectivity tables. Therefore, there is no limit on the size of the mesh it can load assuming there are enough CPUs available, since there is no need to hold global connectivity on master CPU
- Each CPU reads the same set of data (input file) registering all basic objects used in the problem, such as materials, boundary conditions (BC) and mesh descriptors. So all these objects have the same IDs across CPUs. Arrays of mesh variable and connectivity tables are only allocated locally where they are used.
- The code loads multiple grids decomposing them while reading the mesh file using ParMetis [20] tools. Alternatively, the meshes can be assigned to the CPUs by the user.
- Element nodes shared by different CPUs are moved to separate arrays before the main cycle of calculations. An additional force exchange step is done for these nodes at every cycle.
- The code uses global sorting bins to find close external faces. The face sorting can be done in a number of cycles specified by the user. The Common-Plane entity can be created for each pair of close faces if the contact area is positive. If one of

the faces resides on another CPU, then its copy is created and used locally as a ghost face.

- Each external face refers to a face based boundary condition. If two different boundary conditions are assigned at interacting faces then the average parameters are used at the Common Plane working with the faces.

The following steps are done to run a problem:

1) **LOAD INPUT OR RESTART:** Reading data files, allocating structures, generating local connectivity and allocating grid variables

2) **PREPARING FOR THE RUN:** Global space limits are found across all CPUs. They define global orthogonal sorting bins used on all CPUs. Nodes are sorted into the bins and coincident nodes are searched for on each CPU. If such nodes are found they are merged and local connectivity tables are rewritten. All CPUs exchange their bounding boxes, after that the CPUs with overlapping boxes exchange the lists of bins occupied with the nodes. Based on that information nodes shared across CPUs are found and lists of such nodes are created on each CPU. Since element connectivity does not change throughout the computations this step should be done just once before the main cycle.

3) **COMPUTATIONAL CYCLE BEGINS**: All entities (nodes, faces, Common Plane Objects, elements) are sorted if needed. For example, if there are contact boundaries specified in the problem, then external faces, and existing Common Plane Objects are sorted into the bins on each CPU

4) **EXCHANGING FACE CONNECTIVITY DATA BETWEEN CPUS**: CPUs exchange their bounding boxes, then the CPUs with overlapping boxes exchange lists of bins occupied by the faces. The list of CPUs contacting with the given CPU through the faces is created by selecting CPUs with commonly occupied bins. In addition to that the list of overlapping bins is created for each CPU interacting with the given CPU. The array of ghost faces is created. The data for that array will be copied from the other CPUs using the list of contacting CPUs and the list of overlapping bins.

5) **ZERO FORCES**: Nodal forces are set to zero and new variables for the external faces are calculated

6) **APPLYING ELEMENT SOLVERS**: Using current nodal velocities nodal positions are estimated for ½ time step forward, velocity gradient tensor as well as the new cell volume are found, using these quantities the new material state is found for ½ time step forward, internal nodal forces are calculated using newly found cell based stresses and the hourglass forces are added

7) **EXCHANGE FORCES FOR THE NODES SHARED ACROSS CPUS:** Using the list of shared nodes found at STEP 2 each CPU sends and receives the forces for these nodes.

8) **EXCHANGE GHOST FACES DATA**: Coordinates and velocities for the face nodes as well as face masses are sent to other CPUs to update the ghost faces.

9) **CALCULATING CONTACT FORCES:** Generally the code loops on the existing CP entities at each cycle to calculate contact forces but in a number of cycles specified by the user new CP entities can be created. (For example, to model wave propagation through the jointed rock mass it can be done just once since the number of contacts stays the same throughout the calculations but for penetration problems it should be done every 2-4 time steps since the contacts change all the time.) For that purpose all candidate face pairs are looked for in a loop on non-empty sorting bins with the following requirements: the normals for the separated faces point in opposite directions; faces can not belong to the same element; ghost face pairs are excluded (because they are treated on the other CPU). If the area of contact is positive when looking for new CPs, one must check if there is an existing CP separating candidate faces among the CPs sorted into the current space bin (Note that all CPs store information about the contacts including the IDs of faces they separate). If this is no such CP found then a new CP entity is created with a new history, otherwise the existing CP entity is used to store the history variables. The number of history variables stored depends on the contact properties. Usually they include the normal and shear displacements, maximum displacements, shear slip and the forces incremented at the plane each time step

The area of contact and the forces on CP are found using the following steps:

A. coordinates for the face nodes are found at ½ time step using their current coordinates and velocities,
B. trial Point Of Contact (POC) is found as the midpoint of the segment connecting the candidate faces,
C. face projection polygons are found when the nodal coordinates from step A are projected onto the CP with the normal defined as an average normal for the faces,
D. the area of contact is found as intersection of the face projection polygons and final POC is set to the center of gravity of the contact area polygon,
E. the forces are calculated at the plane using contact area, velocity and the history variables. Calculated contact forces at existing or newly found common planes are then distributed to the participating nodes**.** More details can be found in the next paragraph.

10) **BC:** face based boundary conditions (pressure boundary) are applied to add external forces
11) **BC:** node based boundary conditions (velocity or force boundary) are applied to add external forces

12) **UPDATING NODES**: moving nodes to the new locations and update nodal velocities
13) **BACK TO STEP** 3

Contact forces update

Let us consider two interacting faces with the unit normal vectors $\vec{n}_1$ and $\vec{n}_2$ pointing outwards. Figure 1 shows a 2D case. Using current nodal velocities one can advance both faces to ½ time step forward and find A_c, the area of intersection of their projections onto the common plane. The point of contact then is found as the center of gravity for the contact area. We will define the unit normal to the common plane as $\vec{n} = (\vec{n}_1 - \vec{n}_2)/|\vec{n}_1 - \vec{n}_2|$ and the center of the plane as the midpoint of the segment connecting the face centers. The unit normal is updated every time step. Depending on the contact model applied the following history variables may be required for the update:

1) The old unit normal $\vec{n}_{old}$
2) The value of the old normal force F_n and shear forces vector $\vec{F}_s$
3) The maximum normal closure $u_{\max}$
4) The normal closure u
5) The shear displacement u_s
6) The shear slip u_{sp}

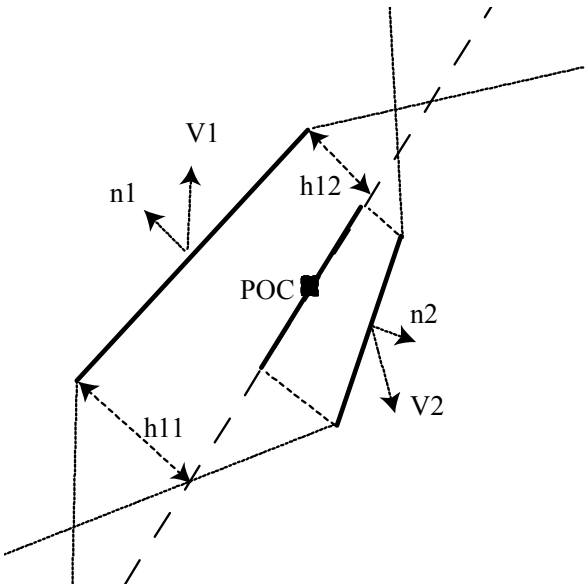

Figure 1. Common plane determination for a pair of faces in 2D. The CP is shown with the dashed line.

The faces are allowed to over penetrate. The penalty force resisting the penetration depends on the value of the penetration called “the normal closure” in a nonlinear way.

Constitutive relations at the contact

Since one of main application of the contact algorithm is to model jointed rock media it is important to capture the main features of the joints. It is known from the experimental observations [16] that the joint closure is a non-linear function of the applied normal stress resembling a hyperbola. Let us assume the following function of form for the normal modulus

$$E = \begin{cases} E_0 \dfrac{a^2}{(a-u)^2}, \dot{u} > 0 \\ E_0 \dfrac{a^2}{(a-u_{\max})^2}, \dot{u} \le 0 \end{cases} \quad (1)$$

Here a is the aperture, u is the normal closure, E_0 is the initial normal modulus and $u_{\max}$ is the maximum closure up to the current time. If integrated for the loading condition it gives the following dependence for the normal stress

$$\sigma_n = \frac{E_0 u}{(a-u)} \quad (2)$$

Contacts are considered to be isotropic with a Coulomb friction law and a limited tensile strength. Thus the shear force at the contact is limited by the yield surface dependent on the normal force as

$$F_{s\max} = CA_c + F_n \tan(\phi) \quad (3)$$

where C is the shear cohesion, A_c is the area of contact and ϕ is the friction angle.

Anytime the yield surface is applied to restrict shear stress (forces) some plastic deformations are accumulated. We will use "shear slip" variable u_{sp} to characterize the amount of plastic deformation at the contact similar to [17]. The increment of the shear slip is expressed as

$$\Delta u_{sp} = \frac{\left\langle |F_s| - F_{s\max} \right\rangle}{GA_c}, \quad (4)$$

where G is the shear modulus.

The friction angle ϕ is changing with the amount of shear slip to account for the softening effect as

$$\phi = \phi_0 + (\phi_0 - \phi_1)\left\langle 1 - u_{sp} / u_{sp\,0} \right\rangle \quad (5)$$

To account for joint dilation due to shear slip ν, the normal force should be adjusted anytime the shear slip is incremented as

$$\Delta v_n = \langle 1 - F_n / F_{cr} \rangle \tan(\Psi_0) \Delta u_{sp}$$
$$\Delta F_n = A_c E \Delta v_n = A_c E \langle 1 - F_n / F_{cr} \rangle \tan(\Psi_0) \Delta u_{sp} \quad (6)$$

where Ψ_0 is the initial dilation angle and F_{cr} is the critical normal force above which dilation will not occur.

The model described above is capable of reproducing the main features of joint response in rocks as it was shown in [17].

Explicit update of contact forces

The normal closure is advanced to the end of the time step as

$$u_n' = u_n + V_n \Delta t \quad (7)$$

The maximum closure for all times is found as

$$u_{n\max} = \max(u_{n\max}, \min(a, u_n')) \quad (8)$$

The normal force is incremented as

$$\Delta F_n = A_c V_n \min\{E(u_{n\max}), E_{\max}\} \Delta t / a \quad (9)$$

where E is the normal modulus which depends of the normal closure.

In the explicit scheme the value of closure in the end of the step is used in the stiffness function. If time step is big enough then the projected closure u_n' may surpass the aperture. In this case a cut-off value $E_{\max}$ is used for the modulus.

The velocity V_n describes relative motion of the faces towards the common plane and is expressed as

$$V_n = \vec{V}_1 \bullet \vec{n} - \vec{V}_2 \bullet \vec{n} \quad (10)$$

where $\vec{V}_1, \vec{V}_2$ are the average velocities of the faces calculated using their nodal velocities.

The shear force is incremented using similar expression

$$\Delta \vec{F}_s = A_c \vec{V}_t G \ \Delta t / a \quad (11)$$

$\vec{V}_t$ is the velocity of the relative motion of the faces parallel to the common plane calculated as

$$\vec{V}_t = \vec{V}_1 - \vec{V}_2 - (\vec{V}_1 - \vec{V}_2) \bullet \vec{n} \quad (12)$$

To exclude incremental rotations of the common-plane, the vector representing the shear force in global co-ordinates is corrected using the old and the new normal vectors as

$$F_{si} = F_{si}^{old} - e_{ijk} e_{kmn} F_{sj} n_m^{old} n_n + \Delta F_{si} \quad (13)$$

After the shear force has been incremented, the yield surface is applied to limit its amplitude as

$$\vec{F}_s' = \vec{F}_s \frac{\left|\vec{F}_s\right|}{F_{s\max}(F_n')} \qquad (14)$$

If the dilation angle Ψ_0 is big, then the maximum shear force $F_{s\max}$ will be changing because of the increase in normal stress due to dilation described by Eq(6). This change should be accounted for by using in Eq.(3) the following corrected value of F_n'

$$F_n' = F_n + \frac{\frac{E}{G}\tan(\Psi_0)\langle 1 - F_n / F_{cr}\rangle(|F_s| - CA_c - F_n\tan(\phi))}{1 + \frac{E}{G}\tan(\Psi_0)\langle 1 - F_n / F_{cr}\rangle\tan(\phi)} \qquad (15)$$

The value of the shear slip increment, consistent with the new normal force F_n', is expressed as

$$\Delta u_{sp} = \frac{\langle |F_s| - CA_c - F_n' \tan(\phi)\rangle}{GA_c} \qquad (16)$$

Once the forces at the plane have been found, they are distributed to the nodes of the interacting faces. There are few ways how it can be done. The method of force distribution proportionally to the node penetration h_{1i} has proved to be robust. In this case the contact force added to the node *i* of the plane 1 is expressed as

$$\Delta\vec{F}_{1i} = -(\vec{F}_n' + \vec{F}_s')\frac{h_{1i}}{\sum_{j=1,m1} h_{1j}} \qquad (17)$$

Forces added to the plane 2 have the opposite sign as

$$\Delta\vec{F}_{2i} = (\vec{F}_n' + \vec{F}_s')\frac{h_{2i}}{\sum_{j=1,m2} h_{2j}} \qquad (18)$$

Distributing forces with the weight proportional to their penetration seems to prevent instabilities at the contact interface.

For the reasons of stability time step should be limited by the following formula

$$\Delta t = \min(\Delta t_e, \frac{C_{safe}a}{\sqrt{E/\rho}}), \qquad (19)$$

where C_{safe} is the safety factor and ρ is the average density of the material separated by the joint. As it is seen from (19), when the joint is closing and $E \to \infty$ the time step would go to zero. That is why this scheme is not appropriate for very strong loadings of the jointed media. For this purpose another more robust implicit scheme has been developed.

Implicit update of contact forces

If the constitutive law for the contact is very stiff, small change in the normal joint closure will cause a dramatic increase in stiffness. This will lead to overestimation of the contact force if the explicit scheme described above is applied.

Let us assume that the contact acts like a non-linear spring connecting two faces. Each face has a mass associated with it. This mass is defined as the mass of the element behind the face divided by the number of element nodes and multiplied by the number of face nodes. However, only a fraction of the face mass is included into consideration. For simplicity this fraction is defined as $f_1 = A_1 / A_c$ for the first face and $f_2 = A_2 / A_c$ for the second face. The motion of each face is controlled by the internal forces from the element F_n^{int} and unknown forces at the contact. Assuming that the faces decelerate during the time step with the force taken from the end of the step gives

$$V_n \Delta t - \frac{(F_n + F_n^{\text{int}} + \Delta F_n / 2)\Delta t^2}{2M_c} = \Delta u_0 - \frac{A_c \Delta t^2 E_0 a^2}{4M_c} \int_{u_0}^{u_0+\Delta u} \frac{du}{(a-u)^2}$$

$$\Delta u_0 - \frac{A_c \Delta t^2 E \Delta u}{4M_c\left(1 - \frac{\Delta u}{(a-u_0)}\right)} = \Delta u \qquad (20)$$

Where $M_c = \frac{M_1 M_2 f_1 f_2}{M_1 f_1 + M_2 f_2}$ and M_1, M_2 are face masses. The resultant internal force is expressed as

$$F_n^{\text{int}} = M_c\left(\frac{\vec{F}_1 \bullet \vec{n}}{M_1 f_1} - \frac{\vec{F}_2 \bullet \vec{n}}{M_2 f_2}\right), \qquad (21)$$

where $\vec{F}_1$, $\vec{F}_2$ are the sums of the internal forces acting on the nodes of the first and the second faces. Note, that the internal nodal forces have been calculated before STEP 9 of the algorithm.

$$\Delta u^2 - \left((a-u_0)\left(\frac{EA_c\Delta t^2}{4M_c}\right) + \Delta u_0\right)\Delta u + (a-u_0)\Delta u_0 = 0, \quad (22)$$

$$\Delta u_0 = V_n \Delta t - (F_n + F_n^{\text{int}})\Delta t^2 / (2M_c),$$

Solving quadratic equation (22) gives the change of the normal closure Δu and the equivalent value of the normal force required to yield the given closure

$$F_n' = 2M_c(V_n \Delta t - \Delta u) / \Delta t^2 - F_n^{\text{int}}, \quad (23)$$

If the contact is very stiff and $a - u_0 \to 0, E \to \infty$, one can find that the solution of the quadratic equation gives $\Delta u \to 0$. The normal force needed to stop relative motion of the faces by the and of the step can be found as

$$F^{\infty}{}_n = 2M_c V_n / \Delta t - F_n^{\text{int}} \quad (24)$$

Eq.() gives the limit of so called "slide line" contact, when the closure is very small but sliding can be big since no friction is applied. This limit can be useful to model very stiff contacts.

The shear force is determined after the normal force has been found using the algorithm described for the explicit update.

Condition of no-shear can be enforced if the shear force is calculated as

$$\vec{F}^{\infty}{}_s = -2M_c \vec{V}_t / \Delta t - F_s^{\text{int}} \quad (25)$$

If the normal force is calculated using Eq.() and the shear force is found using Eq.(25) the contact will behave as tied mesh boundary. This option called here as "sticky contact" is useful, for example, to model continuum using multiple meshes tied along the boundaries.

Accounting for the internal forces during the contact force calculation makes implicit scheme more expensive, because one need to send these forces for each node of the ghost face at STEP 8. A better way of including internal forces into consideration is to correct nodal velocities before STEP 8. In this case both F_s^{int} and F_n^{int} should be set to zero but the nodal velocities used in (10) and (12) need to be adjusted for the internal forces.

Contact options and model parameters

The following contact options are available in GEODYN-L:

- "**Slide Line**" - no shear forces are applied, normal forces are calculated using Eq.()
- "**Sticky contact**" - normal forces are calculated with Eq.() and shear forces are found using Eq.(25)
- **Explicit contact** - constitutive equations for the contact are used in a simple explicit update. Time step is limited by the stiffness of the joints.
- **Implicit contact** – constitutive equations for the contact are used. Kinematics of the faces interactions is accounted for during the update. Therefore the joints do not dictate the time step no matter how stiff they are.

The Table.1 below shows the list of parameters for the contact model specified by the user.

Parameter	**Typical value**	**Name**
a	0.1 mm	Aperture
C	0.001GPa	Shear cohesion
ϕ_0	40	Initial friction angle
ϕ_1	10	Residual friction angle
$G = K_s a$	0.05 GPa	Shear modulus
$E_0 = K_n a$	0.05 GPa	Initial normal modulus
Ψ_0	0-15	Initial dilation angle
$\sigma_{cr} = F_{cr} / A_c$	0.1 GPa	Critical dilation normal stress
u_{sp0}	100.	Shear slip at which friction angle drops to its residual value

Table 1: Parameters used in GEODYN-L contact models

The “slide lines” enforcing non penetration constraint are very often used in contact-impact problems. The “sticky” contact represents the case of very stiff contacts with infinite shear cohesion. It can be used to connect non-matching meshes in FE/FD simulations. In the current framework it is also possible to develop “sleepy” contacts that behave as the “sticky” contact for the intact material and turn into “slide lines” with residual Coulomb friction as material fails. The measures of failure in the separated elements (such as plastic strain, porosity etc) cab be used as the switch in the contact response. This approach can help to model macro fracture and fragmentation activating preexisting contacts.

Examples of simulations

1D wave propagation through a jointed media

To study the effect of joints on wave attenuation for a plane shock wave a 1D problem described below was simulated. Solid material (without joints) was modeled first as a reference case. 100 cells were used for 100 mm long region where the first 10 cells were initialized to 1 km/s velocity.
Free surface boundary conditions were applied from both ends. The material model, described in [18] was used for the limestone with the reference sound speed of 4.5 km/s and the density of 2.6 g/cc. The joints were modeled using both implicit and explicit schemes for three different stiffnesses controlled by the aperture parameter a. Figure 2 shows velocity histories recorded at 80 mm range for the different cases.

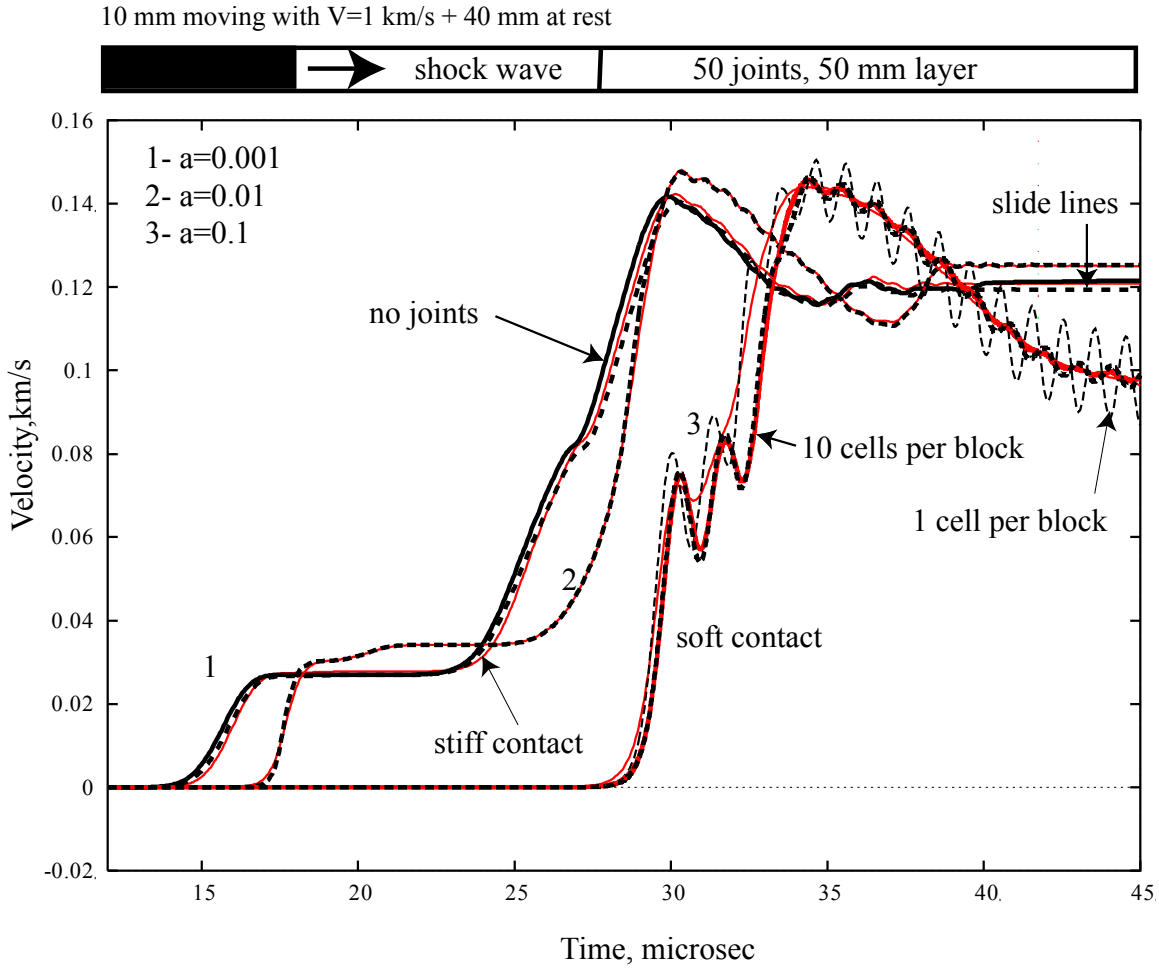

Figure 2. Velocity history for 1 km/s impact of 10 mm layer onto 90 mm layer of jointed rock measured at X=80 mm range: 1-solid material (thick solid line),jointed material with very stiff contacts (thin solid line), jointed material with slide lines(dashed line); 2-jointed material calculated using implicit (solid line) and explicit (thick dashed line) schemes with 1 cell per block;3-jointed material with soft contacts calculated with implicit and explicit schemes and different resolution (1 and 10 cells per block)

The case of very stiff joints (see set 1 in Fig.2) was run only using implicit scheme, since the explicit scheme would require a prohibitively small time step in order to run. In this case the result looks very close to the one calculated for the solid target. The "slide line" contact logic also yields very close results. As the joint stiffness is reduced, the wave travels with slower speeds (see sets 2-3) because of extra time needed to compact the joints. Soft joints also cause more reflection from the block interfaces. It is interesting to note, that the explicit scheme enhances those reflected waves due to systematic overestimation of the contact forces at the interfaces. Increasing the number of cells used per block from one to 10 makes the results of the two schemes close.

2D wave propagation in a jointed media with sticky contacts

By changing contact properties one can get various responses from the jointed media. One of the limiting cases is the "sticky" joint, where material is not allowed to slip and penetrate across the interface. In this case the response of the jointed media should be very close to the material without joints. To illustrate this 2D cylindrical detonation wave has been modeled both on the structured I-J mesh without joints and on an imbricate mesh where blocks where staggered in Y direction (see Fig.3.A mesh on the right)

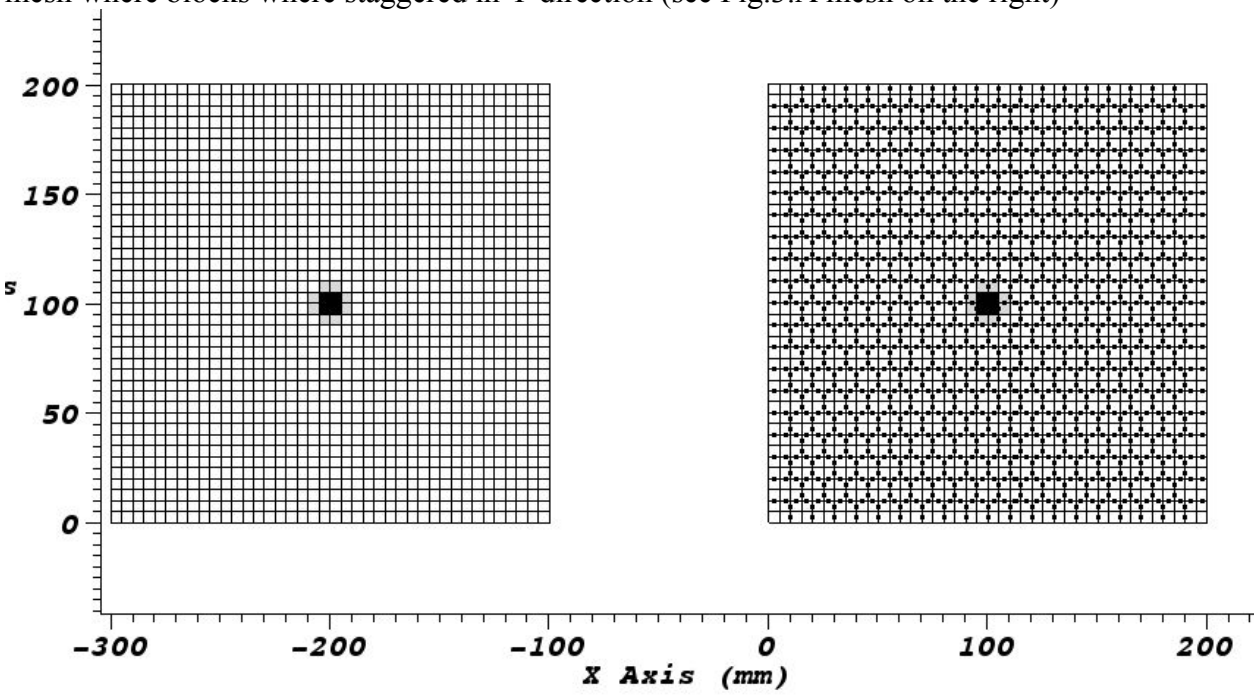

Figure 3. Numerical meshes (A) for a cylindrical detonation wave at different times. Continuum is shown on the left and jointed media with "sticky" joints is shown on the right, the ignition point is shown in the middle.

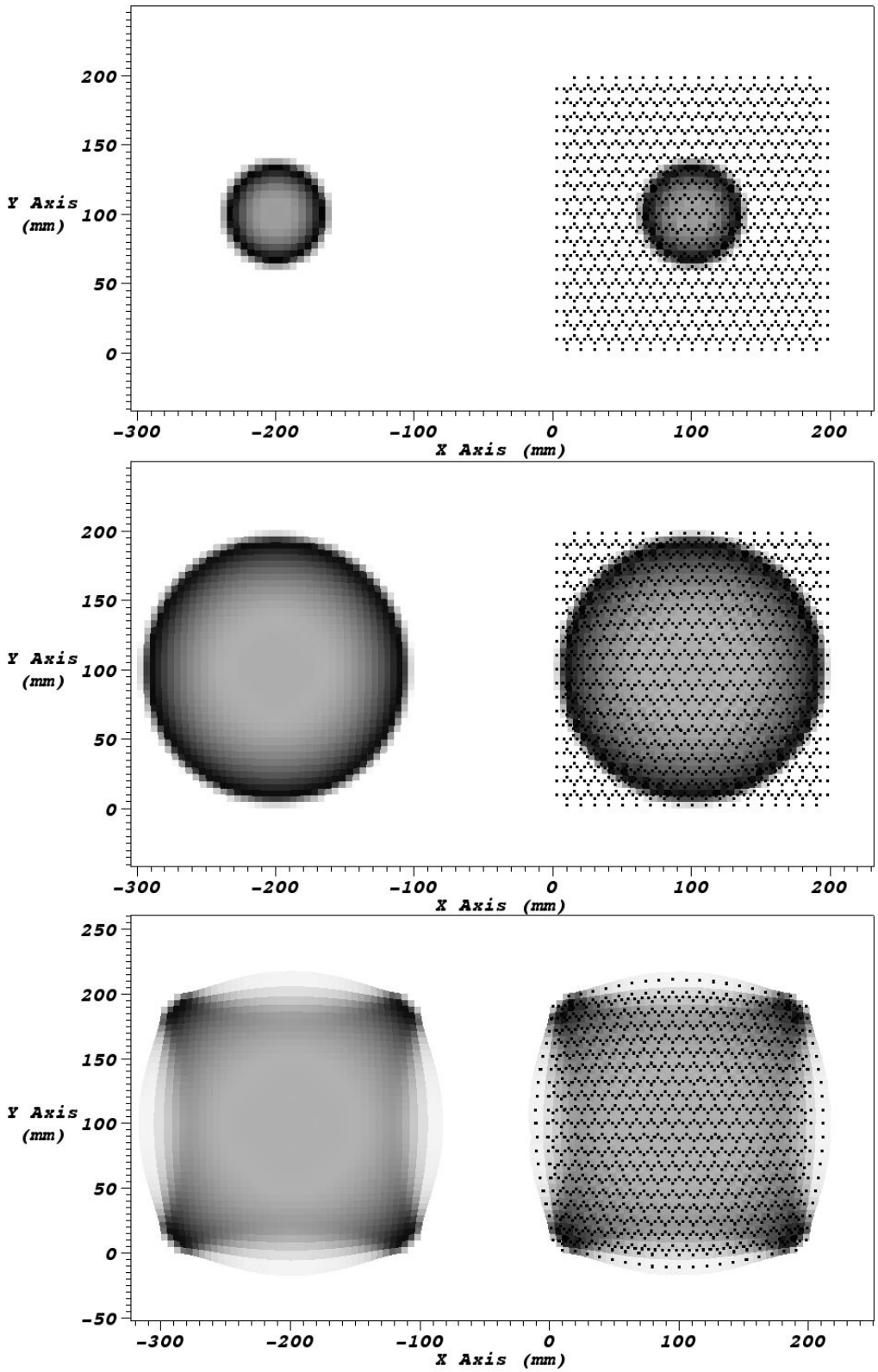

Figure 4. Pressure contours for a cylindrical detonation wave at different times. Continuum is shown on the left and jointed media with sticky joints plotted as dots is shown on the right.

2D block normal impact test: Implicit update vs Explicit update

To test the robustness of both implicit and explicit contact schemes a simple normal impact of two equally sized blocks was simulated using fixed safety factors for the elements. The blocks were meshed differently on purpose to exercise the case when the contact faces are different. The safety factor C_{safe} for the stability of contacts used in (19) was set to a very big number. As a result of this explicit scheme crashed when the problem was run with a typical Courant number S=0.5. When the time step was reduced by a factor of 5 to S=0.1 the scheme still produced unstable results and only a 10 times reduction of the time step (S=0.05) gave results similar to ones produced with the implicit scheme. The following joint properties were used in calculations: a=0.2 mm, E=0.5 GPa, G=0.3 GPa, ϕ_0=38, ϕ_1=38.

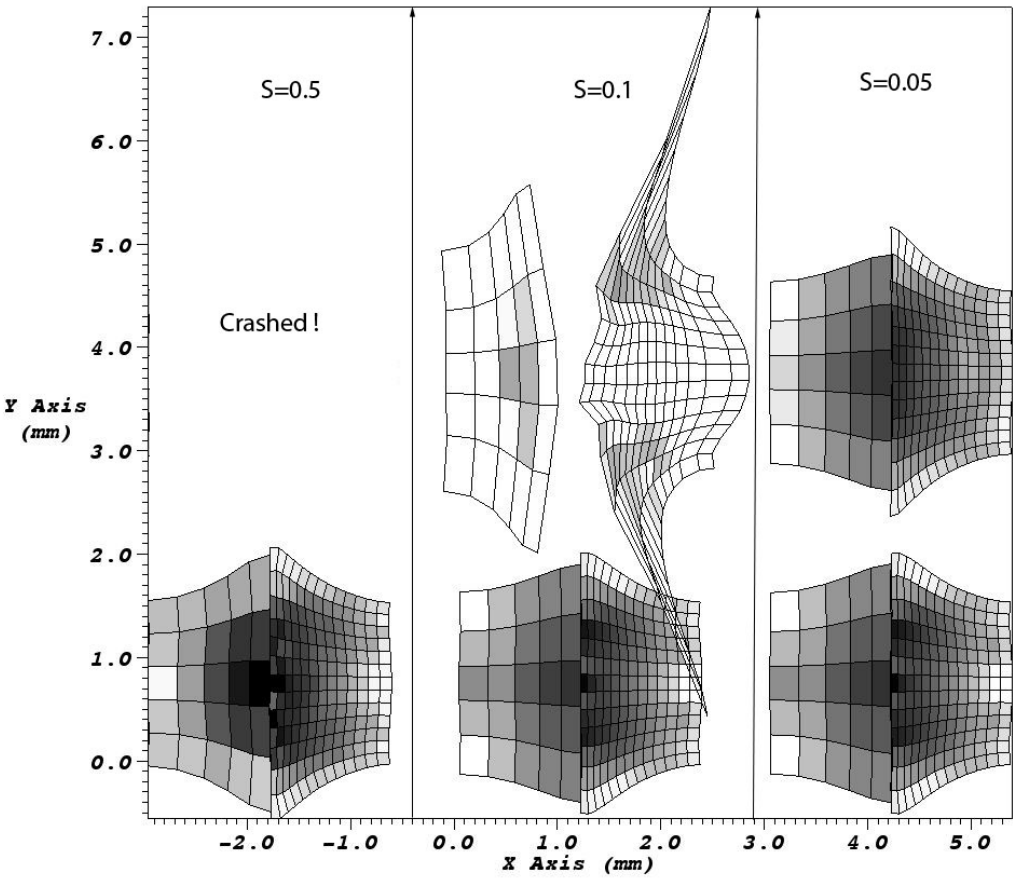

Figure 5. Numerical mesh with the pressure contours for 1 km/s velocity impact of two 1.5x1.5 cm blocks calculated with the implicit (bottom row) and the explicit (top row) schemes with different time step stability factors (0.5,0.1,0.05)

2D block sliding impact test

To test algorithm for the case of non-zero dilation angle a sliding impact of two equal size blocks meshed with 17x17 elements each was simulated using both implicit and explicit updates. The geometry of the problem is shown in Fig.6.The following joint properties were used in calculations: a=0.005 mm, E=0.5 GPa, G=0.5 GPa, ϕ_0=31, ϕ_1=0, Ψ_0=5, F_{cr}=1 GPa. The evolutions of the transmitted normal stress and shear velocity (shown in Fig.7) were recorded at points A and B located in the middle of the contacts in the impacted blocks.

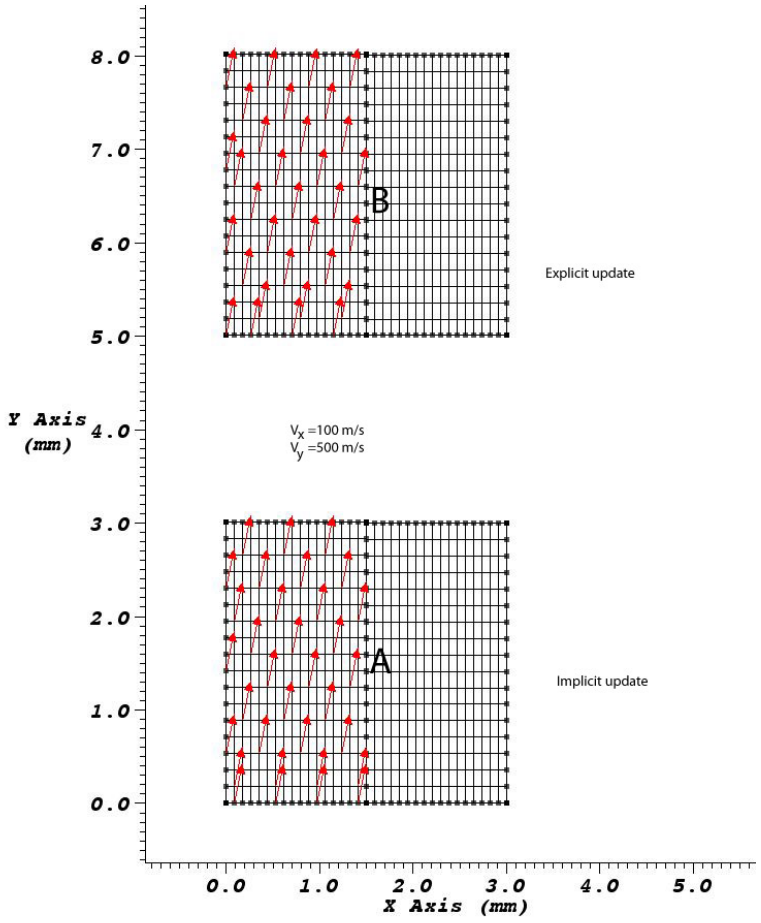

Figure 6. Initial conditions for a sliding impact of two blocks.

Figure 7 demonstrates advantages of using implicit update for the normal force in the case of non-zero dilation at the joints. Both shear velocity and the normal stress are smooth if the implicit update using Eq.(15) is applied (see solid lines). The same variables show some signs of instabilities if the increment for the normal force due to shear slip is calculated using explicit scheme (see dashed lines).

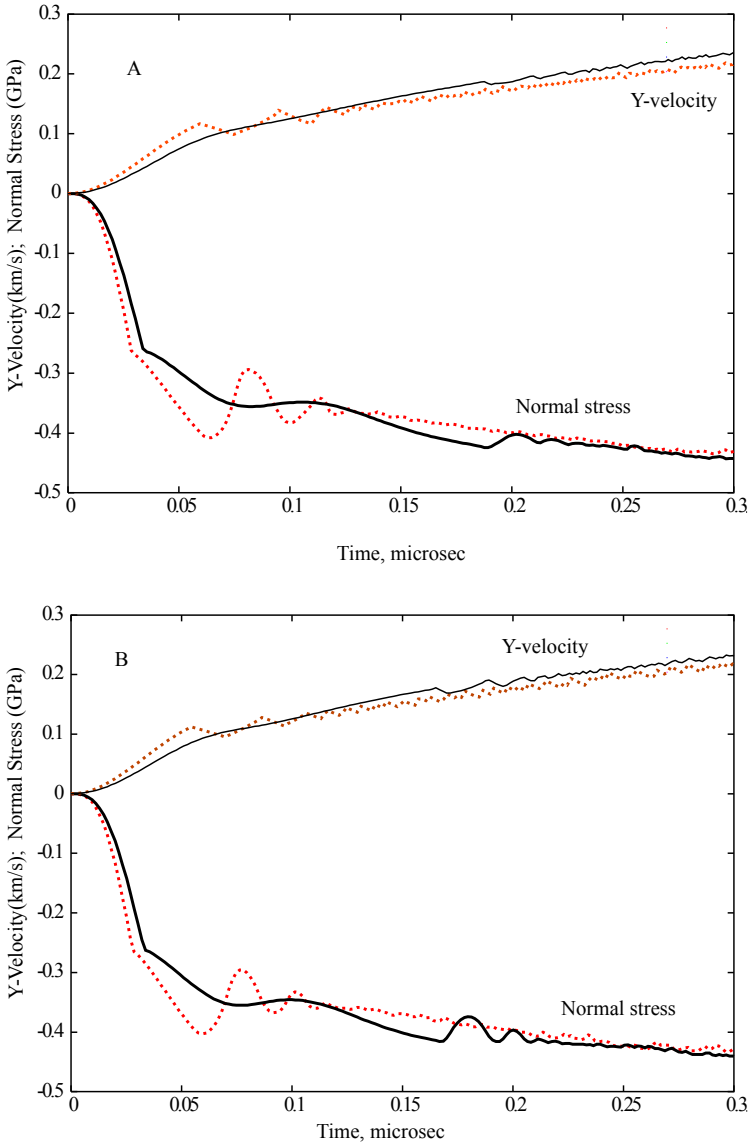

Figure.7 Oblique impact of two blocks: evolution of normal stress and transverse velocity for the implicit (A) and the explicit (B) contacts. Results calculated with the explicit adjustment of the normal contact force for dilation are shown with dashed lines.

2D Projectile penetration through a brick wall

As an illustration of the dynamic contact algorithm in 2D case simulations of a steel projectile penetrating 5 cm thick imbricate wall of concrete at 139 m/s is shown in the figure 8 below. During the penetration of the projectile more and more contacts are activated. Therefore, new Common-Planes were looked for every other time step in order to capture new contacts in time.

The concrete response was modeled with pseudo-cap strength model described in [18]. The model includes effects of hardening due to porous compaction and softening due to

dilatancy. As material softens its tensile strength approaches zero. The consequence of the effect of softening is the presence of elongated elements containing damaged material shown in Fig.9.

A Coulomb friction law was used for the joints. The load-unload curve included one history-dependent parameter, the maximum joint closure, to describe tangent unloading for the joints.

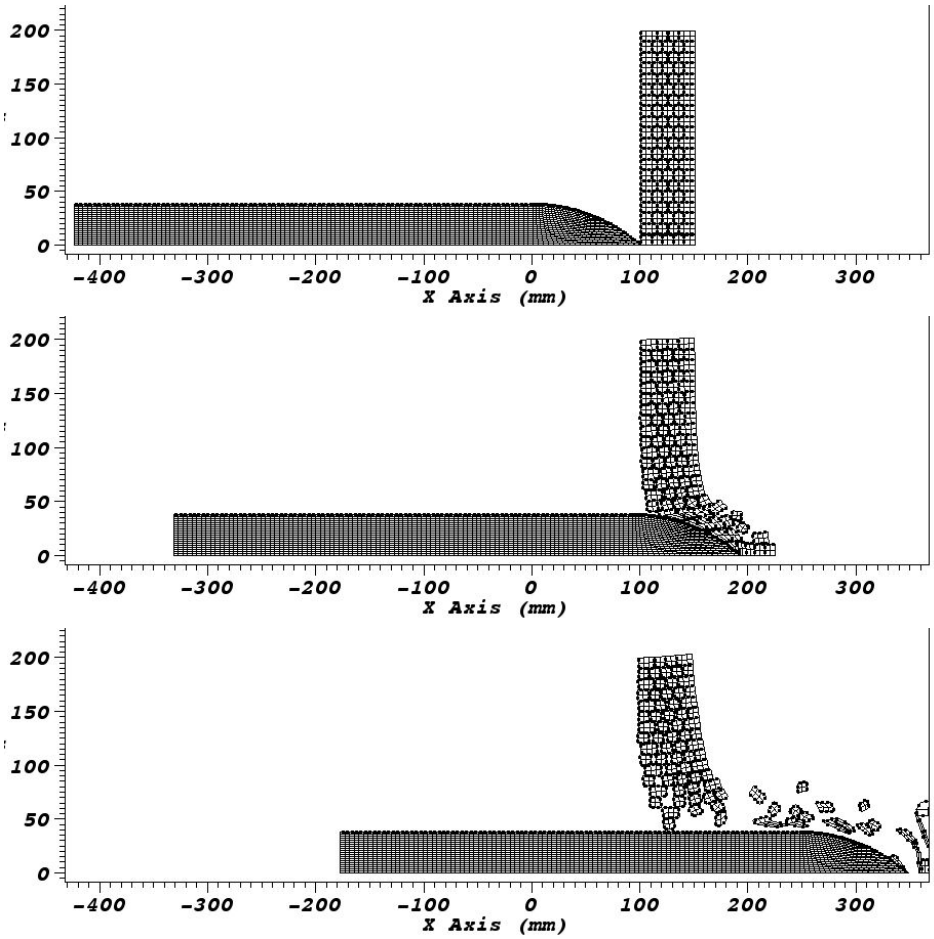

Figure.8 Numerical mesh and contact face locations (black dots) at various times (t=0 ms is at the top, t=0.8 ms in the middle and t=2 ms at the bottom)

It is interesting to note that, because the blocks were allowed to separate, no special technique was needed to prevent mesh distortions which usually takes place in penetration problems.

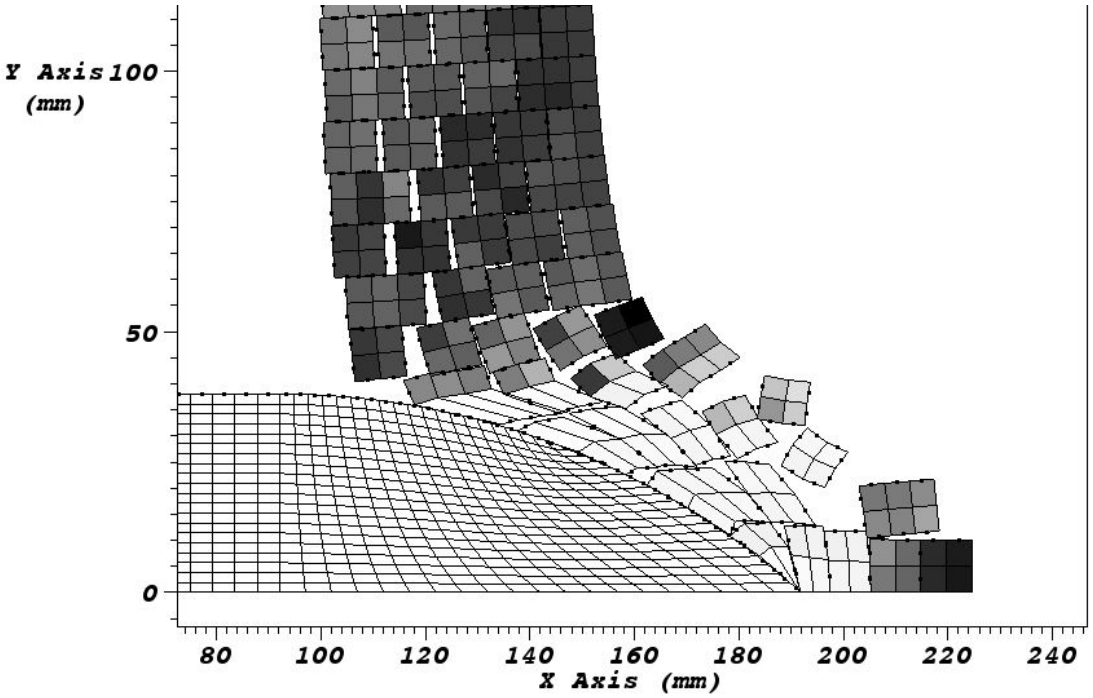

Figure.9 Numerical mesh and tensile strength contours for concrete blocks at t=0.8 ms. White color corresponds to fully damaged concrete.

A bar hitting 3D brick wall

Figure.10 shows results of simulations of a steel 5 m long bar impacting 6.4 x 6.4 x 0.64 m brick wall at 70 m/s. The bar was inclined at 60 degrees. The models described above were used for the concrete and the joints between the bricks.

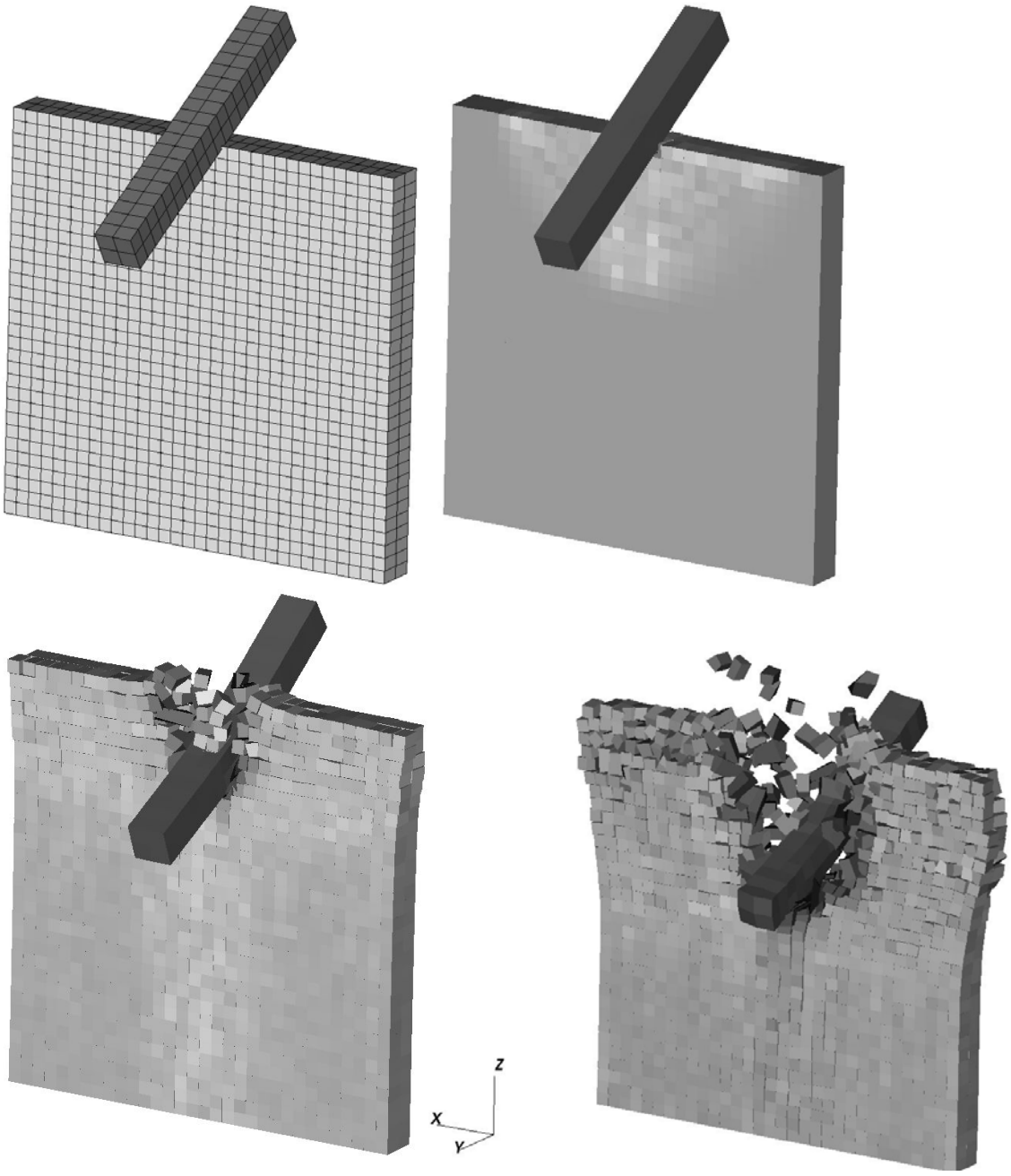

Figure.10 Numerical mesh at cycle zero and contours of tensile strength for brick wall impacted by a steel bar at times 0.0013 s, 0.0183 s and 0.041 s.

Conclusion

- Simple Common Plane (SCP) contact detection technique is very easy and efficient to model all types of contacts (including vertex-to-vertex, edge-to-vertex, edge-to-edge). These cases are modeled by face-to-face contacts using a plane separating the faces (the Common Plane).
- Unlike penalty method traditionally used in FE/FD codes, SCP allows advanced friction laws to be applied at contact surfaces with the history-dependent variables. Such advanced models for the contacts are very important to model heavily jointed rocks and engineering structures with multiple joints.
- In addition to standard stress update used in DEM codes a more advanced quasi-implicit stress update is proposed to avoid time step limitations for the problems with stiff contact law. This method gives the limit of continuum for the very stiff contacts without sliding while the time step is controlled by the elements.
- Parallel SCP algorithm does not provide perfect dynamic load balance for the contacts as, for example, the one described in [4], but it is very generic and easy to implement. The algorithm is completely symmetric and there is no need to specify a master and a slave surface for each time step. Parallelizing the contact amounts to copying the coordinates and velocity of the nodes for the ghost faces which physically reside on other CPUs. There is no need to send the forces calculated at CP to the other CPUs since each Common Plane between the faces resided on different CPUs is duplicated on both CPUs and the forces calculated need only be distributed to the local faces.
- If both DEM and FE methods are used to solve the problem, then applying SCP as contact detection technique in FE is very convenient since both CP and SCP methods use common planes separating interacting entities (blocks, particles, faces of the FE mesh etc.). In this perspective SCP can be looked at as an extension of the traditional CP method used to include FE.

References

1. C.W.Hirt and B.D.Nichols "Volume of Fluid (VOF) method for the dynamics of free boundaries" J.Comput.Phys.,**39**,201(1981)
2. W.Zhu and P.Wang "Finite element analysis of jointed rock masses and Engineering Application" ,*Int.J.Rock Mech.Min.Sci & Geomech.Abstr*.,**30**(5),pp 537-544 (1993)
3. M.Cai and H.Horii "A constitutive model of highly jointed rock masses", *Mechanics of Materials* **13**(1992) pp.217-246
4. W.G. Pariseau "An equivalent plasticity theory for jointed rock masses" , *Int.Journ.Rock Mech and Mining Sci* **36** (1999) pp.907-918
5. T.G Sitharam, J.Sridevi,N.Shimizu "Practical equivalent continuum characterization of jointed rock masses" *Int.Journ.Rock Mech and Mining Sci*. **38** (2001) pp.437-448
6. Desai C.S., Zaman M.M., Lightner J.G. and Siriwardane H.J. "thin-leyer element for interfaces and joints", *Inter.J.Num. Analyt.methods in geomech*.,**8** (1984) pp.19-43
7. Ito M.Y, England R.H. and Nelson R.B. "Computational method for soil/structure interaction probsem", *Computers & Structures* **13** (1981) pp.157-162
8. J.O. Hallquist, G.L.Goudreau and D.J.Benson "Sliding interfaces with contact-impact in large-scale Lagrangian Computations", *Comput.Methods Appl.Mech.Engrg*.**51** (1985) pp.107-137
9. D.J.Benson and J.O.Hallquist "A single surface contact algorithm for the post-buckling analysis of shell structures", *Comput.Methods Appl.Mech.Engrg* **78** (1990) pp.41-163
10. G.Hirota, S Fisher A. State "An improved finite-element contact model for anatomical simulations" *The Visual Computer* (2003) **19**, pp.291-309
11. Heinstein MW, Attaway SW, Swegle JW, Mello FJ (1993) A general-purpose contact detection algorithm for nonlinear structural analysis codes. *Sandia Report*, SAND92-2141UC-705. Sandia National Laboratories Technical Library, Albuquerque, New Mexico
12. T.Peirce,G.Rodrigue "A parallel two-sided contact algorithm in ALE3D", *Comp.Methods Appl.Mech.Engng* (2004)
13. J.Har and R.E.Fulton "A parallel finite element procedure for contact-impact problems", *Eng.with Computers* **19** (2003) pp.67-84
14. Cundall P.A. "Formulation of a three-dimensional distinct element model-part I: a scheme to detect and represent contacts in a system composed of many polyhedral blocks", *Int.J.Rock.Mech Min.Sci&Geomech Abstr* **25**(3) (1998) pp.107-125
15. Nezami E.G. Hashash Y.M.A, Zhao D., Ghaboussi J. "A fast contact detection algorithm for 3-D discrete element method", *Computers and Geotechnics* **31** (2004) pp.575-587
16. S.C. Bandis, A.C.Lumsden, N.R.Barton "Fundamentals of Rock Joint Deformation", *Int.J.Rock Mech.Min.Sci & Geomech.Abstr.*,**20**(6),pp249-268 (1983)
17. J.P.Morris "Review of Rock Joint Models", LLNL report UCR-ID-153650 (2003)
18. O.Yu. Vorobiev, B.T. Liu, I.N. Lomov and T.H. Antoun "Simulation of penetration into porous geologic media ", *Int.J.Impact.Engn*. **34**(4),(2007) pp.721-731

19. S.Plimpton,S.Attaway,B.Hedrickson,J.Swegle,C.Vaughan,D.Garner "Parallel transient Dynamics Simulations: Algorithms for Contact Detection and Smoothed Particle Hydrodynamics", *J.Par.and.Dist.Comp* **50** (1998) pp.104-122
20. Karypis G, Schloegel K, Kumar V ParMETIS 2.0: parallel graph partitioning and sparse matrix ordering library. *Technical Report*, Department of Computer Science, University of Minnesota (1998)
21. J.P.Morris, M.B.Rubin, S.C.Blair,L.A.Glenn, F.E.Heuze "Simulation of underground structures subjected to dynamic loading using the distinct element method" *Engineering Computations*,**21**,pp.384-408 (2004)
22. D.R. Owen,Y.T Feng, E.A.de Souza Neto et all "The modeling of multi-fracturing solids and particulate media", *Int.J.for Numer.Meth.Engng* **60** (2004)pp.317-339